



UNIVERSITY OF LEEDS

This is a repository copy of *Image quality based x-ray dose control in cardiac imaging*.

White Rose Research Online URL for this paper:

<http://eprints.whiterose.ac.uk/84808/>

Version: Accepted Version

Proceedings Paper:

Davies, AG, Kengyelics, SM and Gislason-Lee, AJ (2015) Image quality based x-ray dose control in cardiac imaging. In: Proceedings SPIE 9399, Image Processing: Algorithms and Systems XIII. SPIE Electronic Imaging, 08-12 Feb 2015, San Francisco, California, USA. Society of Photo-Optical Instrumentation Engineers (SPIE) . ISBN 9781628414899

<https://doi.org/10.1117/12.2082795>

Reuse

Unless indicated otherwise, fulltext items are protected by copyright with all rights reserved. The copyright exception in section 29 of the Copyright, Designs and Patents Act 1988 allows the making of a single copy solely for the purpose of non-commercial research or private study within the limits of fair dealing. The publisher or other rights-holder may allow further reproduction and re-use of this version - refer to the White Rose Research Online record for this item. Where records identify the publisher as the copyright holder, users can verify any specific terms of use on the publisher's website.

Takedown

If you consider content in White Rose Research Online to be in breach of UK law, please notify us by emailing eprints@whiterose.ac.uk including the URL of the record and the reason for the withdrawal request.



eprints@whiterose.ac.uk
<https://eprints.whiterose.ac.uk/>

Image quality based x-ray dose control in cardiac imaging

Andrew G. Davies, Stephen M. Kengyelics and Amber J. Gislason-Lee

Division of Medical Physics, University of Leeds, Leeds LS2 9JT, United Kingdom.

ABSTRACT

An automated closed-loop dose control system balances the radiation dose delivered to patients and the quality of images produced in cardiac x-ray imaging systems. Using computer simulations, this study compared two designs of automatic x-ray dose control in terms of the radiation dose and quality of images produced. The first design, commonly in x-ray systems today, maintained a constant dose rate at the image receptor. The second design maintained a constant image quality in the output images. A computer model represented patients as a polymethylmetacrylate phantom (which has similar x-ray attenuation to soft tissue), containing a detail representative of an artery filled with contrast medium. The model predicted the entrance surface dose to the phantom and contrast to noise ratio of the detail as an index of image quality. Results showed that for the constant dose control system, phantom dose increased substantially with phantom size (x5 increase between 20 cm and 30 cm thick phantom), yet the image quality decreased by 43% for the same thicknesses. For the constant quality control, phantom dose increased at a greater rate with phantom thickness (>x10 increase between 20 cm and 30 cm phantom). Image quality based dose control could tailor the x-ray output to just achieve the quality required, which would reduce dose to patients where the current dose control produces images of too high quality. However, maintaining higher levels of image quality for large patients would result in a significant dose increase over current practice.

Keywords: cardiac, x-ray, dose control, image quality.

1. INTRODUCTION

The control of radiographic settings in cardiac x-ray imaging systems is governed by a closed-loop feedback system, referred to as the automatic dose control, ADC. Appropriate settings of the radiographic factors is essential to ensure the safe operation of the x-ray imaging system—the radiation dose delivered to the patient

Send correspondence to AGD: E-mail: a.g.davies@leeds.ac.uk

and staff must be kept to an acceptable level, to reduce the harmful effects of the ionizing radiation exposure, which in extreme cases can result in serious injury.¹ At the same time the imaging system must provide images of adequate quality to allow the clinical task being performed to be completed. In interventional and diagnostic cardiac x-ray imaging systems images are acquired in sequences using relatively high frame rates, typically 15–30 frames per second. The sequences are viewed live, and two modes of operation are available—fluoroscopy and acquisition. Fluoroscopy is a lower dose and lower quality mode used for manipulating interventional devices, positioning of the patient within the image field and so on. In fluoroscopy the images are not normally recorded. Acquisition mode is higher quality (and employs higher radiation dose rates) than fluoroscopy, and most often is used for angiography of the coronary arteries. During the procedure the x-ray tube and image receptor, which are attached to a C-arm, are rotated around the patient to provide projection images taken from different points of view, allowing adequate visualization of the complex three dimensional coronary vasculature.

The automatic dose control must accommodate differences in patients' body habitus, and respond to changes in imaging conditions dictated by the user, such as changes in the projection angle being used or body part being imaged. There are very different thicknesses of tissue in the x-ray beam both between individual patients, but also for a given patient depending upon the x-ray projection. The projection is changed frequently during cardiac x-ray procedures, and therefore the ADC must react quickly to the changes in imaging conditions.

1.1 ADC Operation

A common method of ADC design is for the x-ray system to maintain a constant x-ray dose rate to the x-ray image receptor. The design and implementation of x-ray dose control systems are developed by equipment manufacturers, and comprehensive descriptions of such designs do not exist in the literature. There have been reports that describe the control logic of the some equipment models^{2,3} using phantoms to provoke the ADC to demonstrate its range of responses thus describing how the radiographic factors employed by the units under test respond to different thicknesses of phantom. The ADC changes the tube potential difference (kV), tube current (mA) and pulse duration (ms) according to predefined rules to respond to changing object thickness. Changing the kV alters both the x-ray beam intensity and energy spectra, and changes to the mA and ms result in a proportional change to the beam intensity. In practice, it is common for the ADC to change all three factors during its operation. On all modern systems metal beam filters are also used to further modify the beam's energy profile. On some systems the filter is programmable for a given imaging mode, and on other systems the beam filter is another variable that the ADC can manipulate during its dynamic operation within an image acquisition

sequence.

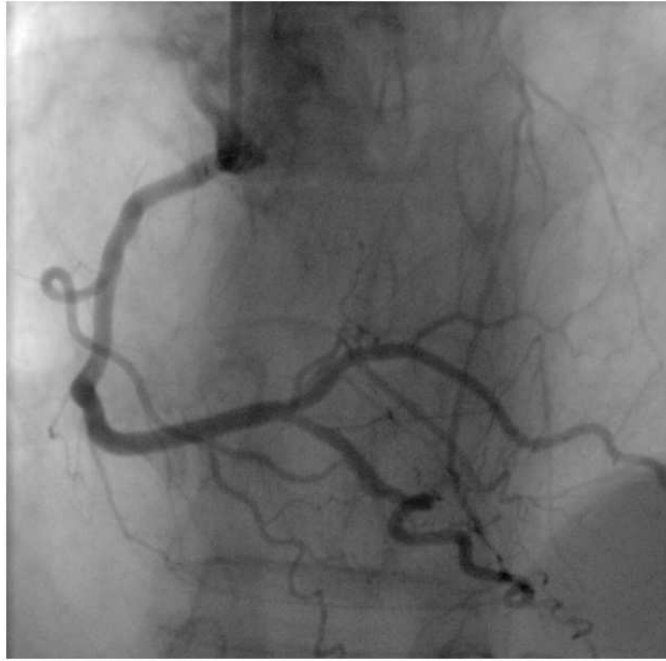
Whilst the previous reports of ADC operation describe the radiographic conditions and resultant entrance surface doses for given phantom thicknesses, they do not describe how the quality of the images that are produced varies with phantom thickness. It has long been known by clinical users that the quality of images is typically better for thinner patients, and falls as a function of patient size. An example is presented in Figure (1), which demonstrates similar imaging geometry images of the right coronary artery from two patients, one a smaller patient, and one a much larger patient, clearly showing superior image quality for the larger patients. The relationship between radiation dose and image quality is complex, although as an approximation, increased radiation dose is associated with improved image quality.

As well as the overall radiation dose used, the quality of the images produced is also affected by the x-ray beam's energy profile, patient thickness and imaging geometry (amongst other factors), therefore the operation of the ADC also plays a key role in quality of images produced. For example the quality of images of a particular sized patient at a given x-ray dose will vary depending on the x-ray beam's energy profile.^{4,5} Current ADC designs seek to maintain a constant dose per frame to at the image receptor, which to a large degree, dictates the level of noise with an image, the contrast of objects within the image will vary considerably. As such, it is important to quantify both the radiation dose and the image quality when describing the operation of an ADC.

Unfortunately measuring the quality of images on a cardiac x-ray system is difficult for end users. There are no accepted standard methods for describing the quality of clinical images, and in any case the variability between patients introduces uncertainty into the findings of such studies. To objectively evaluate images, measurements on images taken of dedicated phantoms are often used, but these measurements must be made on the images prior to the non-linear image enhancement algorithms that are employed in modern x-ray imaging systems, and this type of images are not normally made available to end users. For these reasons descriptions of changes in image quality as a function of patient (or phantom) size are not currently available for cardiac x-ray systems.

1.2 Aims

The aims of this study were twofold— to describe the effect on image quality and dose of a current design of ADC (i.e. one which maintains a constant dose at the image receptor in response to changes in object thickness), and to investigate the result of employing an ADC design that sought to maintain a constant image quality rather than radiation dose to the receptor.



(a) Smaller patient (lower kV)



(b) Larger patient (higher kV)

Figure 1: Two frames from angiograms of the right coronary artery from different sized patients demonstrating the superior image quality produced for the smaller patient.

2. METHODS AND MATERIALS

A software simulation of a simplified x-ray imaging system was created in MATLAB (Mathworks, Natick MA). The simulator was designed to model primary x-ray beam emission in the x-ray tube, attenuation through a phantom representative of a simplified patient, other objects normally found in the x-ray beam (such as the patient couch and anti-scatter grid) and also detection in the x-ray image receptor. For the purposes of this study only the acquisition imaging mode was modelled.

The x-ray source simulated was typical of a cardiac x-ray system, viz. a tungsten anode x-ray tube with an anode angle of 11 degrees, inherent filtration of 3.5 mm Al, constant potential 80 kW generator, operating with a kV range of 40–125 kV. X-ray output spectra were obtained from published sources.⁶ Patients were simulated as simple geometric blocks of polymethylmethacrylate (PMMA) which has similar x-ray attenuation to soft tissue. The thickness of the PMMA phantom was varied to simulate patients of different size. A detail representing a iodinated contrast medium filled blood vessel was also included in the phantom, simulated as a 0.2 mm thick tin object— tin and iodine have very similar x-ray attenuation properties and tin is often used as a substitute in experimental studies for this purpose. The differences in predicted contrast value between tin and iodine objects has been shown to be very small.⁷ Only primary x-ray photons are considered in the simulation. The patient couch was simulated as an attenuator of 3.5 mm thick aluminium. The anti-scatter grid was simulated as absorbing 50% of the primary beam. The x-ray image receptor scintillator was simulated as a 0.55 mm CsI layer. All attenuation data were obtained from published sources.^{6,8} Two ADC schemes were implemented in the model— one that maintained a constant dose per frame at the receptor, and the other which maintained a constant image quality at the detector.

2.1 Model validation

The predictive performance of the model's constant dose ADC was evaluated by comparing ESD and kV predictions against measurements of ESD and reported kV from a reference x-ray system, an Allura FD10 (Philips Healthcare, The Netherlands). The measurements were performed under conditions commonly used for measuring x-ray dose in cardiac x-ray; the source to object distance was 60 cm, a 10 cm gap was maintained between the phantom and the entrance plane of the x-ray detector assembly. For the measurement data the PMMA phantom comprised 30 x 30 x 2.5 cm and 30 x 30 x 1 cm blocks stacked to the desired height. The blocks were placed on top of two wooden spacers on the patient couch, which allowed an ionization chamber to be positioned at the entrance surface of the PMMA blocks. The ionisation chamber used was a 20X6-6 connected to a 2026C

dosimeter (Radcal Corp, Minrovia). Measurements were performed with PMMA phantom thicknesses between 10 and 30 cm in 1 cm increments.

2.2 ADC comparison

Simulations were performed at phantom thicknesses of 15, 20, 25 and 30 cm of PMMA. The source to object distance was set to 70 cm, and the source to image distance adjusted to leave a 10 cm gap between the phantom exit and the receptor. An acquisition rate of 15 frames per second was assumed for dose rate calculations. The simulator predicted the following quantities: phantom entrance surface dose (ESD), and energy deposited in the image receptor's scintillator in the background, b , and in the shadow of the detail, d . Image quality metrics were calculated following the method of Gislason et al.⁷ as follows. The contrast of the vessel was calculated as in equation 1.

$$C = \frac{b - d}{b} \quad (1)$$

Noise was assumed to be poisson distributed, with a mean proportional to the signal level on the detector, and there noise in the image calculated thus:

$$\sigma = \frac{\sqrt{b + d}}{b} \quad (2)$$

The quality of the image was then estimated by the contrast to noise ratio, CNR, i.e. C/σ .

The constant dose ADC varied the x-ray tube potential difference (kV) to achieve a target dose per image at the image receptor. The tube current (mA) and pulse duration (ms) were derived from look up tables based on the kV. The relationships between kV and mA and kV and ms were programmed to be the same as those found on a commercially available cardiac x-ray system (Allura Xper FD10, Philips Healthcare, The Netherlands). The target x-ray dose per frame at the x-ray image receptor was set to 90 η Gy. The radiographic settings and dose rate predicted by the simulator were compared to those measured on the reference x-ray imaging system operating in its default "Left Coronary" acquisition mode using phantoms and imaging geometry matching the simulation.

The second ADC model operated in a similar manner but aimed to achieve a target CNR of the vessel detail. Simulations were performed using two target levels of CNR representing a higher and lower level of quality representing quality predicted to match the constant dose for an average (25 cm thickness equivalent), and larger (30 cm thickness equivalent) phantoms respectively. The CNR dose control was permitted to vary the kV, and used the same kV-mA-ms curves as the constant dose ADC simulator.

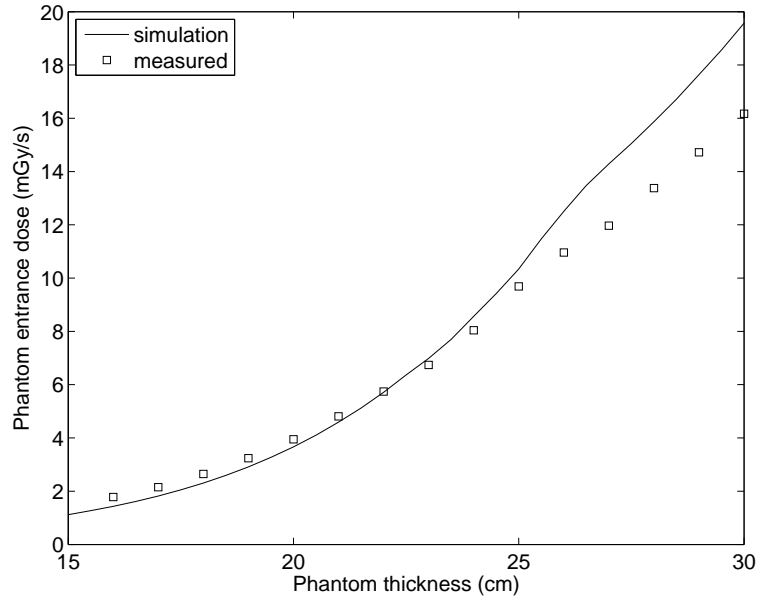


Figure 2: Comparison of simulated and measured entrance surface dose for a range of PMMA phantom thicknesses.

3. RESULTS

3.1 Model Validation

The entrance surface dose and kV predictions of the model closely matched those measured on the reference system, and are shown in figures 2 and 3 respectively.

3.2 ADC Comparison

For both ADC designs there was a non-linear relationship between ESD and phantom thickness. In all cases the ESD rises sharply with phantom thickness, although this rate of rise is considerably higher for the constant quality ADC implementation. The ESD for the constant quality ADCs was highly dependent upon the target image quality. Figure 4 summarises the simulated ESD for the phantom thicknesses studied.

Predicted image quality decreased considerably with increasing phantom thickness for the constant dose ADC. For the constant quality ADCs the target quality was not met for the thickest phantom sizes, as the maximum kV had been reached. These results are summarized in Figure 5.

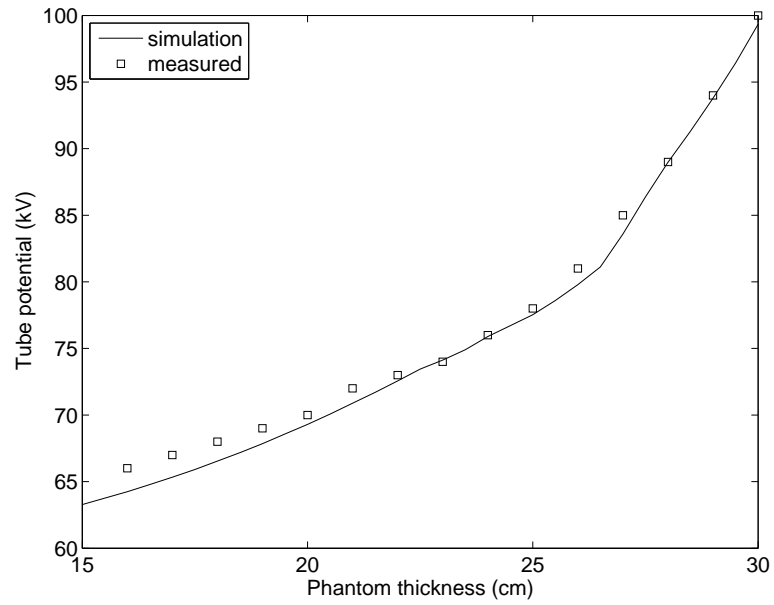


Figure 3: Comparison of simulated and reported kV for a range of PMMA phantom thicknesses.

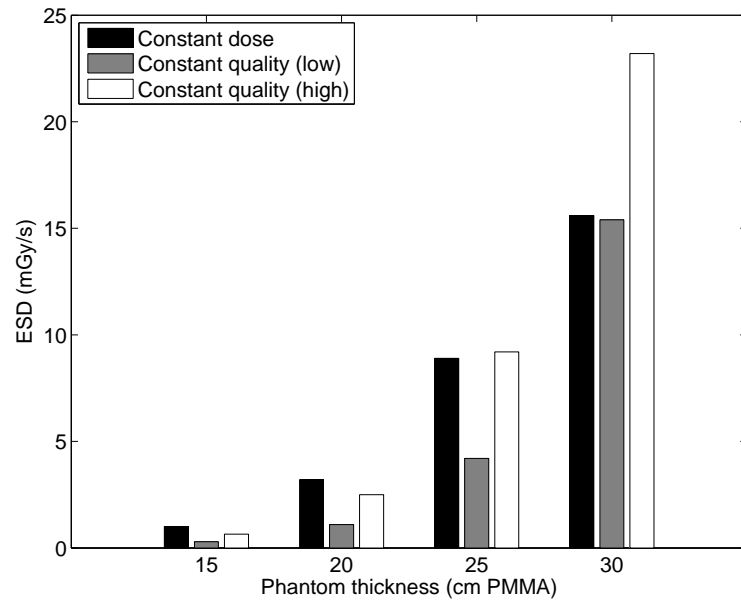


Figure 4: Entrance surface dose rates for the three ADC simulations.

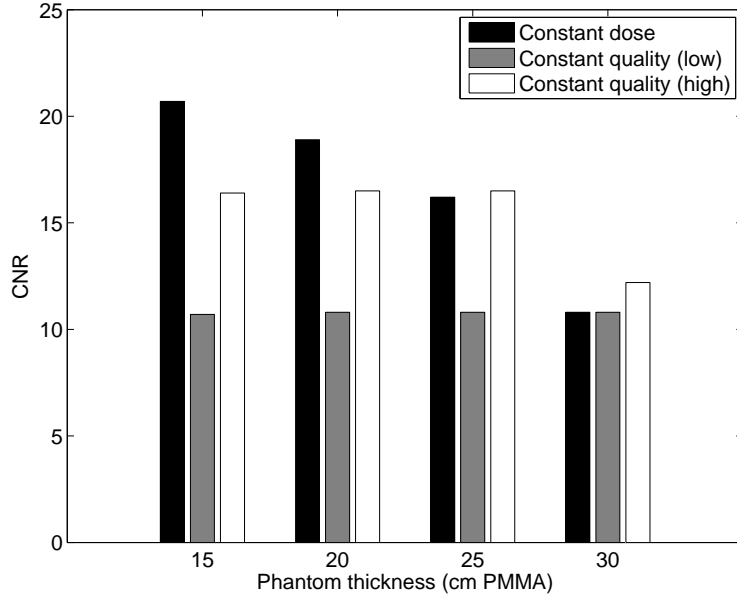


Figure 5: Image quality produced for the three ADC simulations as a function of phantom thickness.

4. DISCUSSION

The dose delivered to patients in medical x-ray imaging should be governed by the ALARA principle— As Low As Reasonably Achievable. On one hand it may be considered that the constant detector dose rate ADC designs do not implement this completely— if the quality of images delivered for larger patients is sufficient for the clinical task, then it could be concluded that the quality of images for smaller patients is too great, and that the image quality for these patients, and therefore radiation dose, could be reduced. Conversely, if the quality required for smaller patients is demand by the clinical task, then there is an argument that the quality provided for larger patients is insufficient, and both quality and therefore dose, should be increased. On the other hand, the term “reasonably achievable” is key to the argument— if the rigid adherence to delivering constant image quality would compromise acceptable ADC response in other respects (e.g. safe radiation control, fast reacting to changing conditions, stable operation, acceptable x-ray tube life, cost and so on), then this would not be “reasonably achievable”. Whilst the constant image quality ADC designs allows a reduction in radiation dose for cases for thinner phantoms, the increase in required dose to achieve the target quality for the thickest patients may be too high for clinical use, and for the thickest phantoms studied the target quality could not be achieved using the maximum kV-mA-ms values allowed in the simulation.

There are a number of challenges in incorporating an image quality based dose control system. In this study a simple computer model was used to calculate contrast to noise ratio for simple assumed objects in the image. Such a computed metric may be too simple to represent a perceived quality of a clinical image— not only were the objects considered in the model simplistic (notably in the use of a uniform background object), but the model used did not account for a number of factors that will affect both patient dose and the quality of delivered image quality, notably scattered radiation, the anti-scatter grid, the temporal response of the image system (such as motion unsharpness), and any image processing which is normally applied to images prior to display. However, a metric of image quality based on the clinical imaging stream is also not without problems— for example, if the clinical images are analysed for the conspicuity of a given object (such as a catheter, guide wire, or contrast agent filled artery) then there will clearly be an issue when the object in question is not in the image field. A hybrid approach using a computer model (whose metrics are always available) updated by real-time analysis of quality on objects in the image field when available, could offer a solution to this problem.

For a given phantom thickness, it is known that different x-ray beam energy profiles can produce images of different quality for the same dose to the phantom.^{5,7} In this experiment the constant quality ADC was constrained to use the same programmed kV-mA-ms curves as measured on the reference clinical system. It is therefore the case that if different kV-mA-ms curves were used (and different beam filters), then the performance of the constant dose ADC would be affected, possibly reducing the phantom doses required to achieve the target image quality.

5. CONCLUSION

X-ray imaging systems must deliver adequate image quality for the clinical task being undertaken, whilst keeping the X-ray dose to patients as low as reasonably achievable. Current designs of x-ray dose control systems seek to maintain a constant dose at the image receptor and we found using this type of ADC that the image quality decreasing with increasing patient size. An image quality normalising ADC could produce a more context aware operation by setting the quality of images to that required to the clinical task, and the level of quality could be tailored to the needs of the operator. By using such a system it is possible that considerable radiation dose savings could be made (reducing harm to the patient) for thinner patients, where the constant dose ADC produced images of a grater quality than necessary. However, maintaining a constant dose for very large patients may result in an unacceptably high radiation dose rate being delivered.

ACKNOWLEDGMENTS

This work has been performed in the project PANORAMA, funded by grants from Belgium, Italy, France, the Netherlands, and the United Kingdom, and the ENIAC Joint Undertaking.

REFERENCES

- [1] Koenig, T. R., Wolff, D., Mettler, F. a., and Wagner, L. K., "Skin injuries from fluoroscopically guided procedures: part 1, characteristics of radiation injury.," *American journal of roentgenology* **177**, 3–11 (July 2001).
- [2] Lin, P.-J. P., "The operation logic of automatic dose control of fluoroscopy system in conjunction with spectral shaping filters," *Medical Physics* **34**(8), 3169 (2007).
- [3] Rauch, P., Lin, P.-J. P., Balter, S., Fukuda, A., Goode, A., Hartwell, G., LaFrance, T., Nickoloff, E., Shepard, J., and Strauss, K., "AAPM Report No. 125: Functionality and operation of fluoroscopic automatic brightness control/automatic dose rate control logic in modern cardiovascular and interventional angiography systems," (2012).
- [4] Tapiovaara, M. J., Sandborg, M., and Dance, D. R., "A search for improved technique factors in paediatric fluoroscopy A search for improved technique factors in paediatric fluoroscopy," *Physics in medicine and biology* **44**, 537–559 (1999).
- [5] Gislason-Lee, A. J., McMillan, C., Cowen, A. R., and Davies, A. G., "Dose optimization in cardiac x-ray imaging.," *Medical physics* **40**, 091911 (2013).
- [6] Sutton, D. and Cranley, K., "IPEM Report 78: Catalogue of Diagnostic X-ray Spectra and Other Data," (1997).
- [7] Gislason, A. J., Davies, A. G., and Cowen, A. R., "Dose optimization in pediatric cardiac x-ray imaging," *Medical Physics* **37**(10), 5258–5269 (2010).
- [8] Hubble, J. and Seltzer, S., "Tables of x-ray mass attenuation coefficients and mass energy-absorption coefficients from 1 keV to 20 MeV for elements $Z = 1$ to 92 and 48 additional substances of dosimetric interest." <http://www.nist.gov/pml/data/xraycoef/> (1996). Accessed 12th Jan 2015.